Supplementary material: Williams et al. (2020)
Methods and Petrographic Descriptions of Selected Chondrules

Overview

Petrographic data on each of ten Allende and nine Karoonda chondrules includes tomographic imaging (CT) of each chondrule in its entirety; electron microprobe (EMP) x-ray intensity maps of polished sections of chondrule fragments, in major and minor elements for 18 chondrules; and quantitative EMP analyses of olivine, pyroxene, mesostasis, and other phases in each section. Quantitative analyses of many silicate phases have been performed and that data is presented in this supplement. Petrographic calculations using x-ray map data include modal analyses of the silicate portions of five Allende chondrules (cf. Ebel et al., 2008, 2016). Measurement of the opaque/silicate volumetric ratio from 3D CT data would be feasible, as would measurement of chondrule diameters and volumes (cf. Ebel and Rivers, 2007). Estimation of the bulk elemental composition of each chondrule would be possible from these data, perhaps as an exercise for the ambitious student. The degree of alteration of each chondrule may be estimated by inspection of BSE images, in which bright (high Z) areas toward rims show post-formation diffusion of Fe into the chondrule.

Methods:

Computed tomography (CT) data were collected as described in Ebel and Rivers (2007). The CT data collected in 2002 and 2003 were reprocessed in 2018 using software running in IDL, circa 2015, written by Dr. Mark Rivers of the Center for Advanced Radiation Sources, University of Chicago at the Advanced Photon Source synchrotron, Brookhaven National Laboratory (DOE) (Rivers, 2012) (http://cars9.uchicago.edu/software/epics/tomoRecon.html, and, more directly relevant, http://cars9.uchicago.edu/software/idl/tomography.html). Reconstructions that took 1-2 hours in 2004 now take seconds. The results today from the data collected so long ago, due to continued improvements by Dr. Rivers, are far superior to those produced earlier.

Reconstructed CT volumes were processed into tiff stacks and avi movies using the free software ImageJ (FIJI) developed by the National Institutes of Health. Because the CT data are 16-bit depth, they have been adjusted (window/level = 3500/7500) to a window of grayscales that seem appropriate. They have been cropped and output as 8-bit images, as well, to minimize file size.

At the time these maps, mosaics, etc. were collected, tools for map combination, phase analysis and other tasks were not yet as prevalent as today. Modal analyses were computed according to methods described by Ebel et al. (2008), and using the modal analysis code provided in this supplement, written in the IDL interpreted high level language, but readily translated into python. Code (in IDL) for mosaiccing multiple maps, cropping, removing 'hot' pixels in element maps, and other functions are available from author Ebel. A script (in Java) for placing registered (correctly stacked) maps and RGB composites from a single folder into correctly labeled Adobe Illustrator layers for post-processing is also available (i.e., for building the AI file layers).

Descriptions of 5 Allende Chondrules:

Allende 4308-chA is a porphyritic olivine-pyroxene chondrule. Euhedral olivine phenocrysts, most <100 μm across, are embedded in mesostasis (15%) containing Ca-rich pyroxene interpreted as a late or quench phase. Smaller, anhedral, patchy Ca-poor pyroxene surrounds olivine grains, and is more abundant toward the chondrule rim. Large (up to 250 μm diameter), sub-round metal+sulfide nodules are scattered throughout, and silicates toward the chondrule rim are enriched in FeO. The distribution and abundance of these opaque, high-density nodules are evident in CT data. Nodules are heterogeneous in Fe, Ni and S, and are rimmed by a Ca-, P-rich, Si-free phase, probably a phosphate. Nodules contain irregular mixtures of nearly pure Fe metal; FeNi metal alloy; and Fe-, Ni-sulfide. Merrillite - $Ca_3(PO_4)_2$ - crystallizes at ~1973 K, well above Fe metal (1800 K), and troilite (~1200 K), and nodules are rimmed by Ca-depleted pyroxene. This suggests a cooling sequence in which exsolved, partially molten Fe-Ni-S-P nodules solidified after mesostasis, leaching Ca from glass to form phosphate, and re-equilibrating below the solidus of the Fe-Ni-S mixture. Element maps reveal Mn concentrated in quench mesostasis phases (Ca-rich pyroxene), and Cr absent from olivine and mesostasis glass, low in orthopyroxene, higher in mesostasis quench phase (Ca-rich pyroxene) and concentrated in small fractures in olivine. Na is below detection in olivine, Ca-poor pyroxene, and the Ca-rich pyroxene inferred as a mesostasis quench phase, but uniform in mesostasis glass, and enriched in a less abundant, Al-rich quench (or alteration) phase (nepheline $NaAlSiO_4$ or sodalite $Na_8(AlSiO_4)_6Cl_2$?). Cr is absent in olivine and groundmass; present, but not strongly correlated with Ti or Fe in pyroxene; and strikingly zoned in spinels, which have Cr-poor cores and Cr-rich rims throughout the chondrule. Mn is slightly enriched in pyroxene, relative to other phases, and not strongly correlated with Fe overall.

Allende 4327-ch1 is a barred olivine chondrule with large (up to 250 μm diameter), sub-round metal+sulfide nodules are scattered throughout, and silicates toward the chondrule rim are enriched in FeO. Mesostasis (17%) contains Ca-rich pyroxene interpreted as a late or quench phase, always nucleating on olivine. In polished section, two barred domains are visible, and also a region with coarser, more euhedral olivine that appears to be a recrystallized domain that is chemically almost identical to the barred domains. There is a slight textural difference in Cr distribution between this domain, in Cr mapping, and the more regular barred domains. This third domain may represent a collisional event experienced by the chondrule. Closely-spaced olivine bars (10-50 μm wide) are distinguishable in CT images. Element mapping shows that Cr is nearly absent in olivine grains, but concentrated along small fractures in olivine. A sharp circular boundary (2560 μm diameter) inside the outermost textural boundary, is visible in the Cr map (Fig. 8). Where it is observable, this boundary corresponds to the outer extent of most of the barred olivine, where it gives way to the coarsely crystalline to massive olivine rim of the chondrule. No Al-rich mesostasis extends beyond this boundary. The very small Cr-bearing grains dispersed on this boundary are also visible in the back-scattered electron (BSE) image (Fig. 9), but not against the background of other phases in the Fe map at 5 μm spatial resolution. This chemical-textural phenomenon suggests that Cr-bearing metal was deposited on a perfectly spherical, rapidly quenched barred olivine chondrule, which is the core object here, prior to formation of the igneous olivine rim that

lies beyond the Cr-rich grains. Distribution of Mn, by contrast, shows no relationship to textural features.

Allende 4327-ch2 (not used in the present study) is an Al-rich chondrule (Type C) or olivine-bearing CAI. Groundmass (glass, or a cryptocrystalline melilite-feldspar mixture) surrounds abundant Cr-, Fe-bearing $MgAl_2O_4$ spinel; highly anhedral forsteritic olivine; and an Al-, Ti-bearing Ca-free silicate, possibly orthopyroxene. A Ca-free, Na-bearing Al-silicate is particularly abundant toward the chondrule rim, possibly nepheline $NaAlSiO_4$ or sodalite $Na_8(AlSiO_4)_6Cl_2$. Occurrence of this phase is correlated with increased Fe content of local silicates and spinel in elemental maps. Cr is absent in olivine and groundmass; present, but not strongly correlated with Ti or Fe in pyroxene; and strikingly zoned in spinels, which have Cr-poor cores and Cr-rich rims throughout the chondrule. Several spinels apparently (in 2D section) included in olivine (poikilitically) are also Cr-bearing, and Cr is not enriched in any apparent micro-cracks. Such cracks only appear in the groundmass. Mn is slightly enriched in pyroxene, relative to other phases, and not strongly correlated with Fe overall. Na is below detection in olivine and Ca-poor pyroxene; at uniformly low abundance in groundmass; and enriched in Na-silicate (sodalite?) which has sharp boundaries against the other phases. No strong Na diffusion into groundmass is evident, although Na is concentrated along some micro-cracks in the section. This chondrule appears to have been quenched from a very Ca-depleted liquid at high temperature, and Fe and Na were introduced from the chondrule exterior at high temperature.

This chondrule contains many grains of a titanian Ca-poor pyroxene with the approximate formula $Ca_{0.02}Mg_{1.65}Fe_{0.01}Cr_{0.03}Al_{0.48}Ti_{0.06}Si_{1.71}O_6$. Such a pyroxene would represent an excursion beyond known pyroxene composition space (Cameron and Papike, 1980; Sack and Ghiorso, 1994, 2017), and deserves further study.

Allende 4327-ch5 is a porphyritic olivine-pyroxene chondrule. Most of the large, euhedral to subhedral Ca-poor pyroxenes (2.4wt% FeO) include rounded olivine grains that are strongly zoned in FeO, increasing to 11 wt% FeO at pyroxene contacts. Mesostasis does not contact olivine anywhere, and contains numerous 1-10 μm silicates, including Ca-rich pyroxene and a Na-rich phase. Rounded FeS nodules, associated with minor Fe-Ni-S patches, are common on and just inside the chondrule rim. Mesostasis (15%) and silicates are heterogeneous in FeO content, and Fe is concentrated along numerous veinlets throughout the chondrule. These are *not* the same veinlets, confined to olivine grains, upon which Cr is concentrated in x-ray maps, in otherwise nearly Cr-free olivine (Fig. 10). The origin of the microfractures in what appear to be relict (embayed, very rounded, enclosed in pyroxene) olivine grains is not clear. No such veinlets are present in the orthopyroxene that encloses the olivines. If these olivine grains pre-date the chondrule-forming event [REF: Jones, Steele on relict OL], then the Cr in them should also. By contrast, the Mn in this chondrule is concentrated very strongly in the Ca-rich pyroxene in the mesostasis (Fig. 11). Sodium is concentrated in the mesostasis, and there is no evidence for strong core-rim zoning of Na, which, if present, would indicate significant lower-temperature nebular or parent-body alteration. This is a thermally mature chondrule that records multiple heating events. It experienced sufficient durations

of heating to form very large, homogeneous phenocrysts of orthopyroxene almost completely absorbing earlier-formed, earlier-fractured olivine, but not in equilibrium with them in Fe (Fig. 12). Cooling was slow enough that many crystals grew in the mesostasis.

Allende 4448-ch1 is a perfectly spherical, barred olivine chondrule. Bars (~50 μm wide) are broken into linear chains of euhedral olivine (segmented). Small sulfide grains are scattered through the chondrule in the mesostasis. Mesostasis contains Ca-rich pyroxene and very small quench crystals identified as C-poor and Ca-rich pyroxene, nucleating on olivine. Olivine bars are not distinguishable in CT images. Element maps reveal that Mn is present in mesostasis quench phases and olivine, and slightly enriched in Fe-, S-rich patches, but very low in mesostasis glass. Cr is uniformly concentrated in mesostasis and its quench phases, and very low in olivine. Cr is very concentrated where slightly curved fractures pass through olivine grains but not through surrounding glass. Maps in Na indicate that Na is concentrated in mesostasis glass, with no apparent concentric zoning of Na in the chondrule.

Table 1: Chondrule mass, type, CT scan date and resolution (micron), and diameter calculated from CT data. Mass for 4308-chA was not recorded.

label	mass (g)	type	CT-date	CT: mu/pxl	D(mu)
4308-chA	-	POP	Apr-02	5.848	2544
4327-ch1	0.043	BO	Nov-03	6.211	2925
4327-ch2	0.007	C	Nov-03	3.876	1868
4327-ch5	0.026	POP	Nov-03	6.186	2314
4448-ch1 (chA)	0.041	BO	Nov-03	6.073	2617

Modal abundances of phase were determined by counting pixels in x-ray intensity maps (Figures, 1-5). Maps of Fe, S, Ca, Mg, Si and Al were combined algebraically. Holes and cracks were not counted. Thresholds applicable to particular phases were determined by visual examination of these maps, were then applied to the entire sample to segment mineral areas, and to count the numbers of pixels attributable to each mineral. Results are presented in Table 2. The pixel identification algorithms that yield modal abundances also produce false-color maps, in which the identified pixels are coded by phase type. Results for two chondrules are shown in Figs. 6 and 7.

Semi-quantitative (uncalibrated) X-ray intensity maps for Mn, Cr, Na, Ti and other elements were also obtained on some chondrules, and sub-areas were mapped at 1 micron/pixel resolution. Quantitative electron microprobe analyses of phases are reported in Table 3 for linear arrays of 1 μm diameter spots, and in Table 4 for single10 μm spots, all labeled on Figures 1-5.

Based on 2D modal analyses and silicate phase analyses, bulk compositions were calculated for all chondrules except 4327-ch5, which contains very coarse-grained and highly zoned phenocrysts. Results are presented in Table 8.

Table 2: Modal abundance (area %) of minerals in 5 chondrule polished sections (See table S4 in ChondruleData_19july2019.xlsx).

	4308-chA	4327-ch1	4327-ch2	4327-ch5	4448-ch1
micron/pixel	4	2	2	3	3
pixels counted	197396	259590	245910	129222	256525
FeS	1.42	5.21	1.42	2.75	2.37
metal	2.49	-	0.08	0.22	0.65
carbonate	0.03	0.00	0.00	0.01	0.10
olivine	38.25	48.19	7.49	11.60	42.87
opx	31.86	9.38	14.19	61.80	29.29
cpx	8.26	7.25	-	7.54	13.68
glass	16.23	17.27	-	14.85	9.64
spinel	-	-	16.67	-	-
groundmass	-	-	31.60	-	-
Na-, Al-silicate	-	-	5.34	-	-
unidentified	1.45	12.70	23.20	1.23	1.39

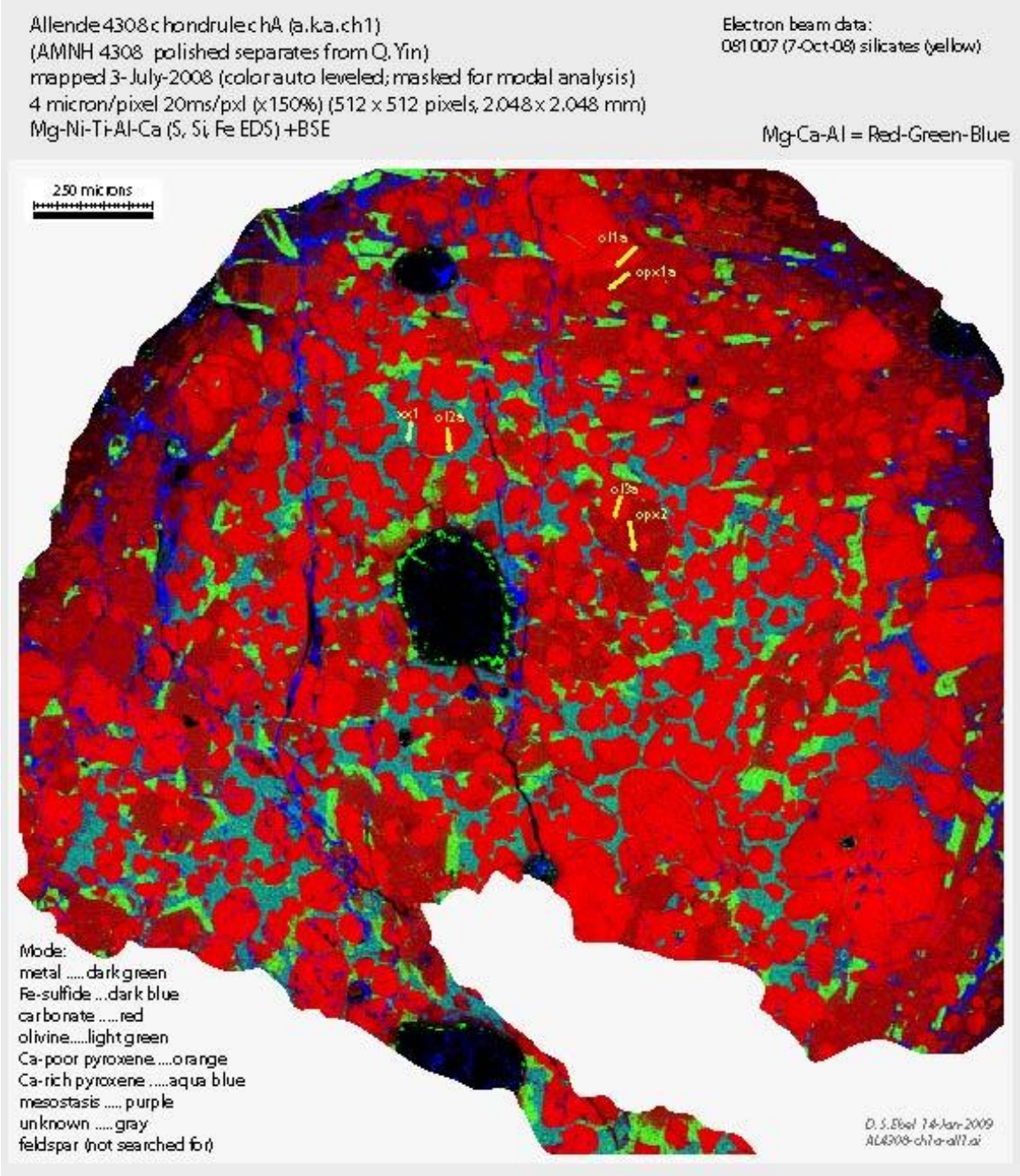

Figure 1: Chondrule 4308-chA, Mg-Ca-Al = Red-Green-Blue x-ray composite map.

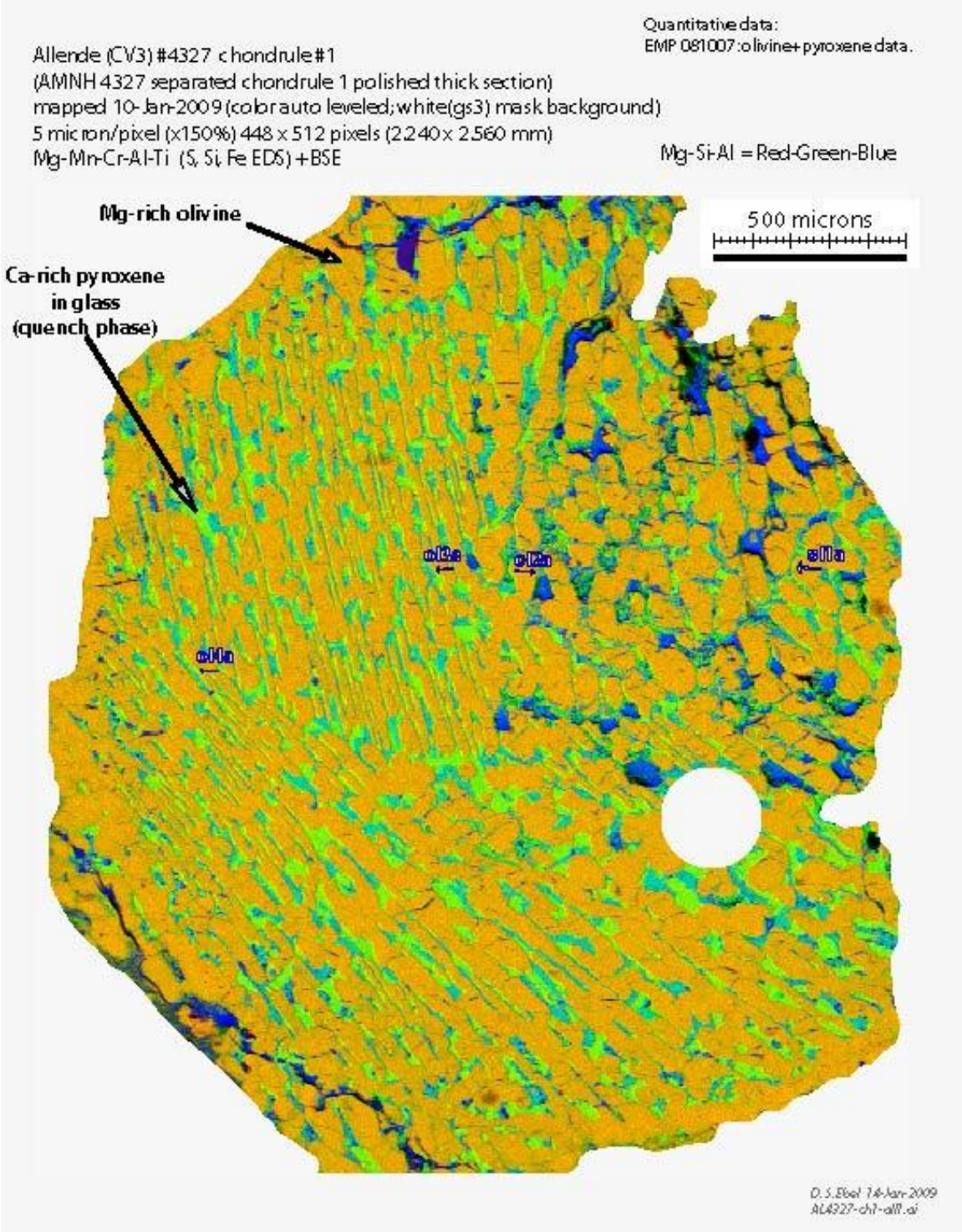

Figure 2: Chondrule 4327-ch1, Mg-Si-Al = Red-Green-Blue x-ray composite map.

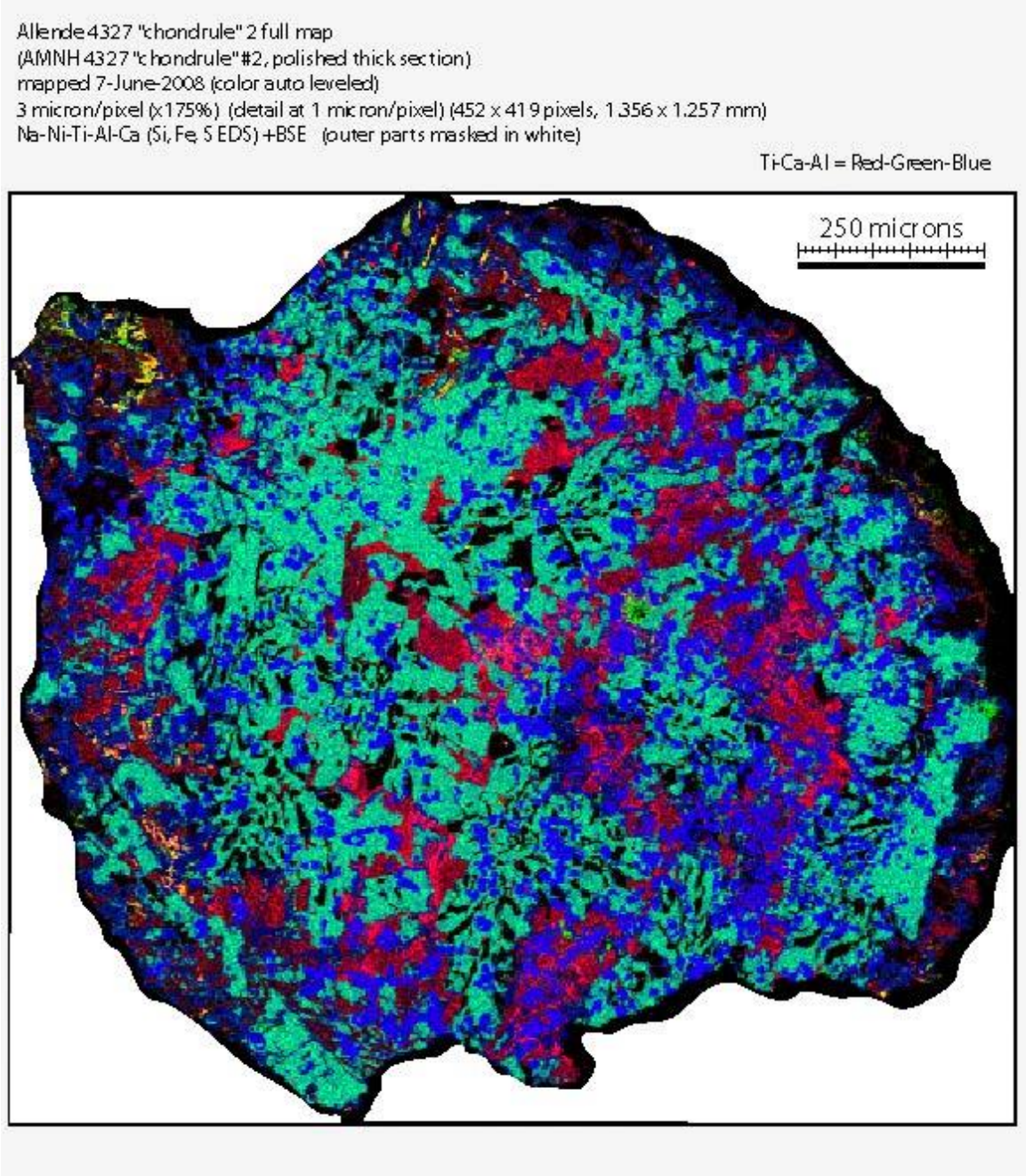

Figure 3: Chondrule 4327-ch2, Ti-Ca-Al = Red-Green-Blue x-ray composite map.

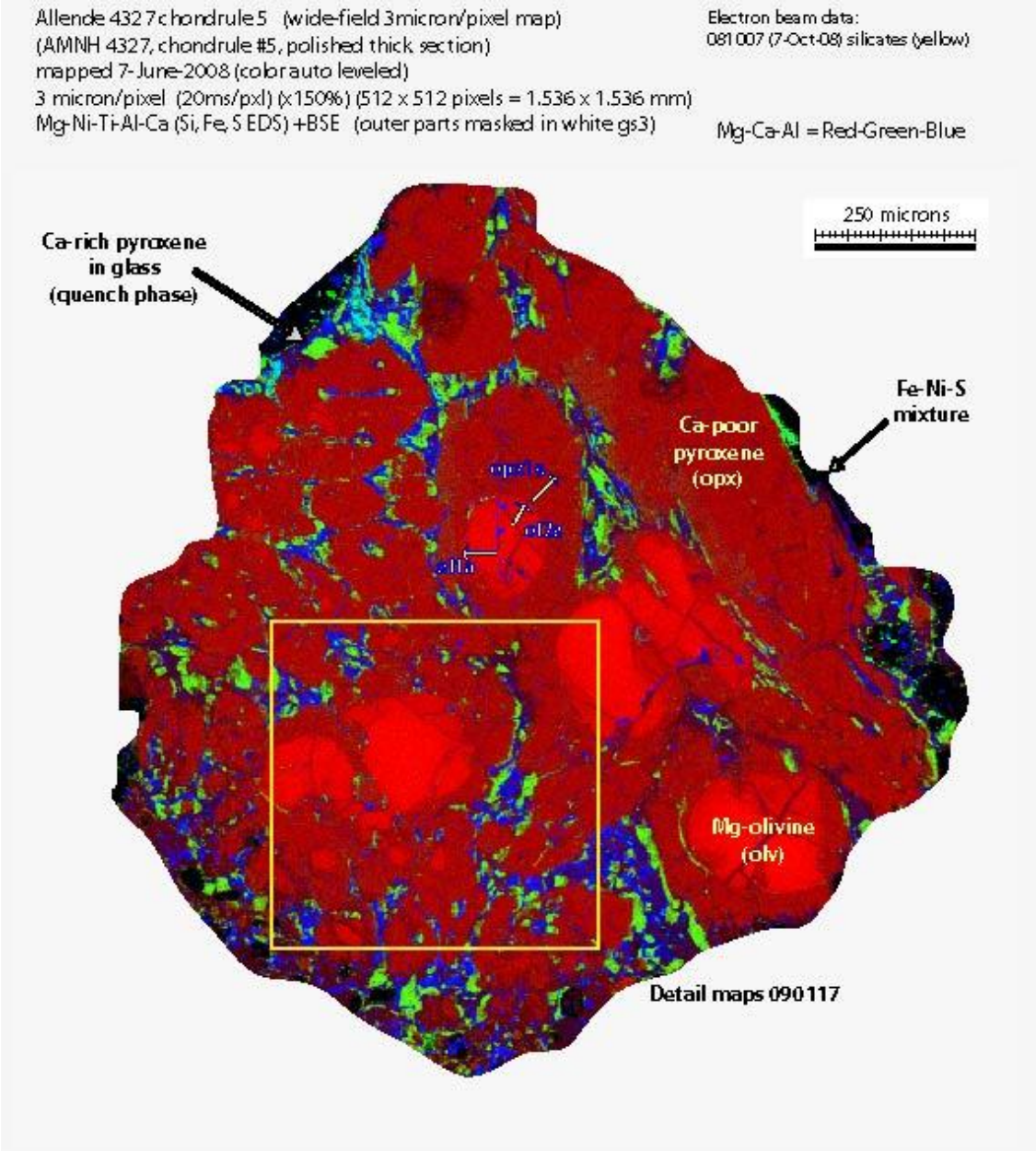

Figure 4: Chondrule 4327-ch5, Mg-Ca-Al = Red-Green-Blue x-ray composite map.

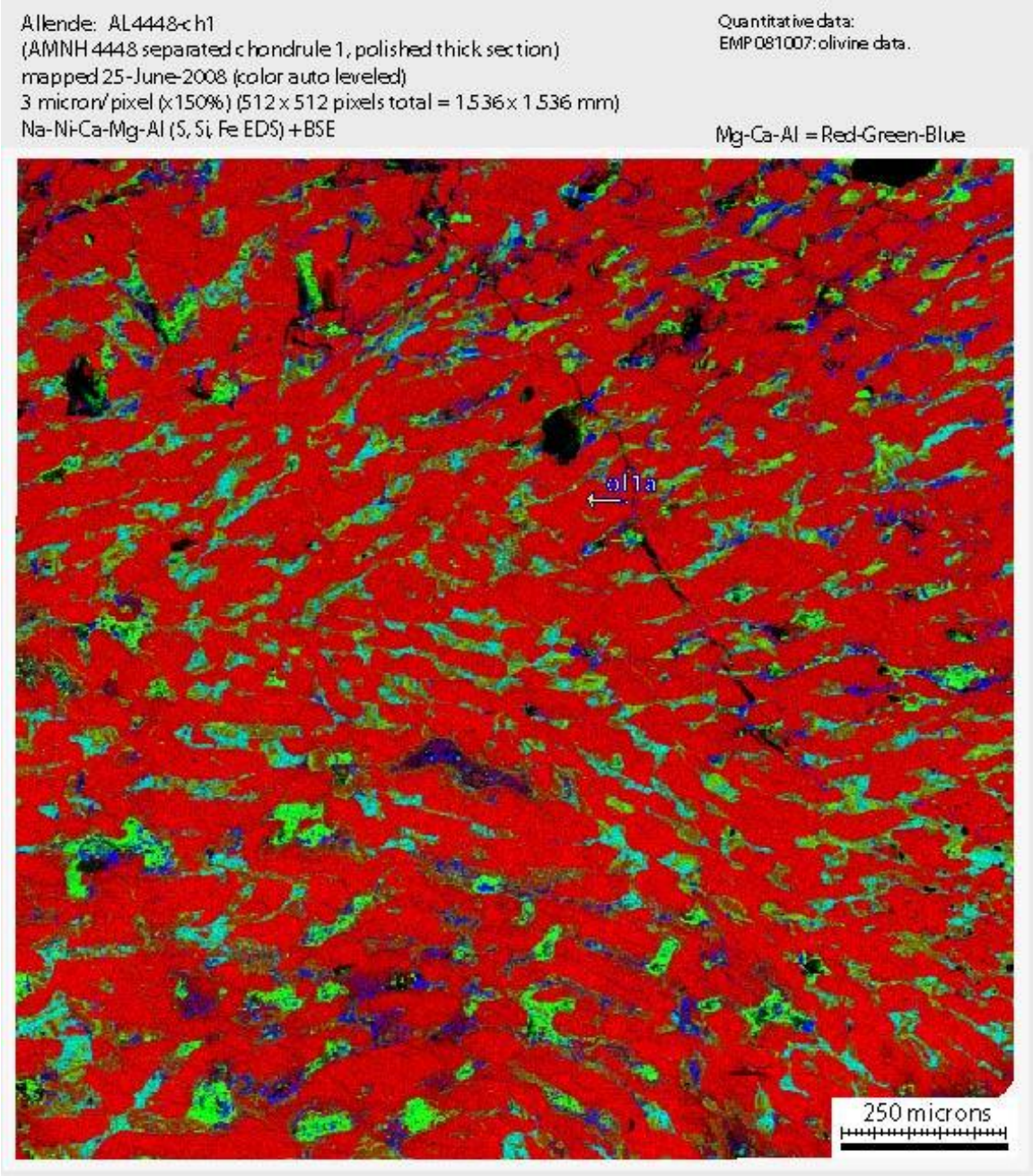

Figure 5: Chondrule 4448-ch1, detail, Mg-Ca-Al = RGB x-ray composite map.

Table 3: Electron microprobe data, 1 micron beam diameter.

n	Comment	total	SiO2	TiO2	Al2O3	Cr2O3	FeO	MnO	MgO	NiO	CaO	Na2O	K2O
19/3.	AL4308-chA-ol1a	100.88	41.5251	0.01524	0.00785	0.04093	9.12494	0.06744	49.883	0.0053	0.20524	0.00867	0.0012
19/4.	AL4308-chA-ol1a	101.04	41.8721	0.01369	0.00259	0.0396	8.00068	0.07831	50.8006	0.02728	0.19737	0	0.0089
19/5.	AL4308-chA-ol1a	100.99	41.9033	0.00341	0.00898	0.04082	7.51503	0.06835	51.1629	0.04018	0.22843	0.01169	0.0067
	count:	3	3	3	3	3	3	3	3	3	3	3	3
	average:	100.97	41.77	0.01	0.01	0.04	8.21	0.07	50.62	0.02	0.21	0.01	0.01
	stdevp:	0.06	0.17	0.01	0.00	0.00	0.67	0.00	0.54	0.01	0.01	0.00	0.00
22/1.	AL4308-chA-ol2a	100.66	42.18	0	0	0.06062	5.48215	0.19984	52.4933	0.06446	0.17481	0	0
22/2.	AL4308-chA-ol2a	100.95	42.419	0.01236	0	0.04356	5.46626	0.17625	52.5957	0.03472	0.19898	0.00001	0
22/3.	AL4308-chA-ol2a	101.10	42.3789	0.01614	0	0.05786	5.86323	0.20964	52.3483	0.01144	0.18804	0.01991	0.0053
22/4.	AL4308-chA-ol2a	101.03	42.1185	0.00014	0.0237	0.07384	7.12522	0.212	51.2186	0.06893	0.18022	0.00815	0.0017
	count:	4	4	4	4	4	4	4	4	4	4	4	4
	average:	100.93	42.27	0.01	0.01	0.06	5.98	0.20	52.16	0.04	0.19	0.01	0.00
	stdevp:	0.17	0.13	0.01	0.01	0.01	0.68	0.01	0.55	0.02	0.01	0.01	0.00
23/1.	AL4308-chA-ol3a	100.38	42.4074	0.00642	0.01515	0.0952	5.5447	0.17692	52.0394	0.00418	0.07461	0.0126	0.0022
23/2.	AL4308-chA-ol3a	101.04	42.378	0.01952	0.02229	0.12992	5.43283	0.20954	52.69	0.02205	0.10193	0.02448	0.0125
23/3.	AL4308-chA-ol3a	100.83	42.0904	0	0.0018	0.05289	6.29947	0.21012	51.9978	0.01557	0.15161	0.00741	0
	count:	3	3	3	3	3	3	3	3	3	3	3	3
	average:	100.75	42.29	0.01	0.01	0.09	5.76	0.20	52.24	0.01	0.11	0.01	0.00
	stdevp:	0.28	0.14	0.01	0.01	0.03	0.38	0.02	0.32	0.01	0.03	0.01	0.01
ALL	**AL4308-chA-olivine**		SiO2	TiO2	Al2O3	Cr2O3	FeO	MnO	MgO	NiO	CaO	Na2O	K2O
	count:	10	10	10	10	10	10	10	10	10	10	10	10
	average:	100.89	42.13	0.01	0.01	0.06	6.59	0.16	51.72	0.03	0.17	0.01	0.00
	stdevp:	0.21	0.28	0.01	0.01	0.03	1.23	0.06	0.88	0.02	0.05	0.01	0.00
	Formula:		1.007	0.000	0.000	0.001	0.132	0.003	1.843	0.001	0.004	0.000	0.000
	Mg# = Mg/(Fe+Mn+Mg+Ni+Ca):		**0.93**										
20/1.	AL4308-chA-opx1a	101.45	59.3234	0.12723	0.89362	0.84586	2.28022	0.15832	37.4255	0.02097	0.34716	0.02082	0.0053
20/2.	AL4308-chA-opx1a	100.96	59.1054	0.11694	0.858	0.87525	2.32713	0.1433	37.1743	0.01144	0.34196	0.00756	0
20/3.	AL4308-chA-opx1a	101.41	59.3383	0.10943	0.82443	0.86959	2.27418	0.14912	37.4737	0.01945	0.34207	0.00973	0.0034
20/4.	AL4308-chA-opx1a	100.83	58.937	0.12007	0.80485	0.8786	2.23846	0.13357	37.3479	0.00191	0.35495	0.00417	0.0046
20/5.	AL4308-chA-opx1a	100.97	59.1416	0.09588	0.71771	0.86288	2.29125	0.13627	37.3425	0	0.36453	0.01013	0.0024
	count:	5	5	5	5	5	5	5	5	5	5	5	5
	average:	101.12	59.17	0.11	0.82	0.87	2.28	0.14	37.35	0.01	0.35	0.01	0.00
	stdevp:	0.26	0.15	0.01	0.06	0.01	0.03	0.01	0.10	0.01	0.01	0.01	0.00
24/1.	AL4308-chA-opx2a	100.73	59.0055	0.20442	1.33124	1.00827	2.33463	0.14939	36.3177	0.0065	0.36881	0.00502	0
24/2.	AL4308-chA-opx2a	99.48	57.3742	0.17053	2.34307	0.97296	2.5064	0.18015	35.3108	0.00841	0.55516	0.05788	0
24/3.	AL4308-chA-opx2a	100.50	58.5273	0.18232	1.27463	1.00486	2.23046	0.15931	36.7335	0	0.38942	0.00304	0
24/4.	AL4308-chA-opx2a	100.86	58.6798	0.17917	1.25383	1.02065	2.20003	0.15125	36.9229	0.02792	0.41826	0.00222	0
24/5.	AL4308-chA-opx2a	100.90	58.8649	0.17808	1.25474	1.01835	2.22198	0.17448	36.7963	0	0.38462	0.00961	0.0015
	count:	5	5	5	5	5	5	5	5	5	5	5	5
	average:	100.50	58.49	0.18	1.49	1.01	2.30	0.16	36.42	0.01	0.42	0.02	0.00
	stdevp:	0.53	0.58	0.01	0.43	0.02	0.11	0.01	0.59	0.01	0.07	0.02	0.00
ALL	**AL4308-chA-opx**		SiO2	TiO2	Al2O3	Cr2O3	FeO	MnO	MgO	NiO	CaO	Na2O	K2O
	count:	10	10	10	10	10	10	10	10	10	10	10	10
	average:	100.81	58.83	0.15	1.16	0.94	2.29	0.15	36.88	0.01	0.39	0.01	0.00
	stdevp:	0.52	0.54	0.04	0.45	0.07	0.08	0.01	0.63	0.01	0.06	0.02	0.00
	Formula:		1.977	0.004	0.046	0.025	0.064	0.004	1.848	0.000	0.014	0.001	0.000
	Mg# = Mg/(Fe+Mn+Mg+Ni+Ca):		**0.96**	# = Al/(Si+Ti+Al+Cr):		**0.02**	Mg# = Mg/(Fe+Mn+Mg+Ni+Ca):			**0.01**			
21/2.	AL4308-chA-xx1a	101.67	56.0222	0.68455	20.8997	0.31547	1.71899	0.28241	5.66057	0.03102	12.0387	4.01535	0
21/3.	AL4308-chA-xx1a	101.76	55.7431	0.77856	19.7355	0.35734	2.29218	0.40072	6.30517	0.0586	12.4307	3.65994	0
21/4.	AL4308-chA-xx1a	101.42	55.2223	0.72337	20.4959	0.30784	2.19776	0.3089	5.77229	0.04197	12.5169	3.82161	0.0144
21/5.	AL4308-chA-xx1a	101.12	53.8077	0.68079	22.0524	0.32754	2.59061	0.24931	5.35405	0.00945	12.0756	3.96018	0.0111
	count:	4	4	4	4	4	4	4	4	4	4	4	4
	average:	101.49	55.20	0.72	20.80	0.33	2.20	0.31	5.77	0.04	12.27	3.86	0.01
	stdevp:	0.25	0.85	0.04	0.84	0.02	0.31	0.06	0.34	0.02	0.21	0.14	0.01

n	Comment	total	SiO2	TiO2	Al2O3	Cr2O3	FeO	MnO	MgO	NiO	CaO	Na2O	K2O
14/1.	AL4237-ch1-ol1	100.90	40.5091	0.06715	0.01396	0.07565	16.2215	0.26308	43.5348	0.01955	0.18284	0.00826	0
14/2.	AL4237-ch1-ol1	100.29	40.0224	0.1196	0.05712	0.12569	16.5874	0.2794	42.8375	0	0.25744	0.00628	0
14/3.	AL4237-ch1-ol1	100.57	40.0074	0.04907	0.02983	0.0813	16.259	0.28228	43.5422	0.00752	0.30823	0.00288	0
14/4.	AL4237-ch1-ol1	101.31	40.2724	0.05034	0.06504	0.07445	17.1839	0.2494	43.143	0.00714	0.2592	0.00054	0.0005
	count:	4	4	4	4	4	4	4	4	4	4	4	4
	average:	100.77	40.20	0.07	0.04	0.09	16.56	0.27	43.26	0.01	0.25	0.00	0.00
	stdevp:	0.38	0.21	0.03	0.02	0.02	0.39	0.01	0.29	0.01	0.04	0.00	0.00
15/1.	AL4237-ch1-ol2a	101.26	39.9004	0.03776	0.03651	0.08331	16.3955	0.29737	44.2059	0.02445	0.2688	0	0.0052
15/2.	AL4237-ch1-ol2a	100.91	39.8453	0.11946	0.09582	0.22719	16.0152	0.25147	43.9943	0.02483	0.31407	0.01918	0.0066
15/3.	AL4237-ch1-ol2a	100.56	40.2705	0.03649	0.03701	0.11552	16.137	0.27853	43.3556	0	0.32515	0	0
15/4.	AL4237-ch1-ol2a	100.75	40.6755	0.0273	0.05802	0.10636	15.7851	0.25182	43.5137	0.02108	0.30013	0.00852	1E-05
	count:	4	4	4	4	4	4	4	4	4	4	4	4
	average:	100.87	40.17	0.06	0.06	0.13	16.08	0.27	43.77	0.02	0.30	0.01	0.00
	stdevp:	0.26	0.33	0.04	0.02	0.06	0.22	0.02	0.35	0.01	0.02	0.01	0.00
16/1.	AL4237-ch1-ol3a	100.95	40.268	0.0635	0.10221	0.08814	16.4804	0.25729	43.4662	0	0.20247	0.01554	0.0024
16/3.	AL4237-ch1-ol3a	101.04	39.9531	0.06301	0.0221	0.09535	16.851	0.28176	43.525	0.00301	0.2312	0.00569	0.0045
	count:	2	2	2	2	2	2	2	2	2	2	2	2
	average:	100.99	40.11	0.06	0.06	0.09	16.67	0.27	43.50	0.00	0.22	0.01	0.00
	stdevp:	0.04	0.16	0.00	0.04	0.00	0.19	0.01	0.03	0.00	0.01	0.00	0.00
17/1.	AL4237-ch1-ol4a	100.50	39.9003	0.05172	0.0416	0.05942	16.592	0.28938	43.2771	0.03694	0.23722	0.01014	0.0007
17/2.	AL4237-ch1-ol4a	100.78	39.8212	0.07258	0.09723	0.1332	16.3737	0.28449	43.6963	0.02262	0.27914	0.00118	0
17/4.	AL4237-ch1-ol4a	101.06	39.9673	0.07246	0.05622	0.12574	16.3398	0.291	43.9555	0.01358	0.22751	0	0.0081
17/5.	AL4237-ch1-ol4a	101.28	40.0382	0.06404	0.03244	0.09215	16.3598	0.27839	44.1589	0.01131	0.23883	0	0.0026
	count:	4	4	4	4	4	4	4	4	4	4	4	4
	average:	100.90	39.93	0.07	0.06	0.10	16.42	0.29	43.77	0.02	0.25	0.00	0.00
	stdevp:	0.29	0.08	0.01	0.02	0.03	0.10	0.00	0.33	0.01	0.02	0.00	0.00
18/1.	AL4237-ch1-ol5a	100.53	38.7573	0.02274	0.06102	0.17098	19.5138	0.65417	41.0824	0.02695	0.21635	0.00907	0.0157
18/2.	AL4237-ch1-ol5a	100.20	39.5	0.02841	0.08251	0.20335	16.6818	0.36358	43.0507	0.02028	0.25936	0.00828	0
	count:	2	2	2	2	2	2	2	2	2	2	2	2
	average:	100.36	39.13	0.03	0.07	0.19	18.10	0.51	42.07	0.02	0.24	0.01	0.01
	stdevp:	0.17	0.37	0.00	0.01	0.02	1.42	0.15	0.98	0.00	0.02	0.00	0.01
All AL4237-ch1-olivine:													
	count:	16	16	16	16	16	16	16	16	16	16	16	16
	average:	100.80	39.98	0.06	0.06	0.12	16.61	0.30	43.40	0.01	0.26	0.01	0.00
	stdevp:	0.33	0.42	0.03	0.03	0.05	0.81	0.09	0.70	0.01	0.04	0.01	0.00
	scratch (wt% / MW):		0.67	0.00	0.00	0.00	0.23	0.00	1.08	0.00	0.00	0.00	0.00
	scratch (+ charges):		2.6617	0.0030	0.0033	0.0046	0.4624	0.0086	2.1534	0.0004	0.0092	0.0002	0.0001
	Formula:		1.003	0.001	0.002	0.002	0.349	0.006	1.623	0.000	0.007	0.000	0.000
	Mg# = Mg/(Fe+Mn+Mg+Ni+Ca):		**0.82**										

n	Comment	total	SiO2	TiO2	Al2O3	Cr2O3	FeO	MnO	MgO	NiO	CaO	Na2O	K2O
31/1.	AL4327-ch5-ol1a	101.12	41.8819	0.03602	0.10308	0.17187	5.83532	0.14509	52.6305	0.00539	0.30847	0	0.0039
31/2.	AL4327-ch5-ol1a	101.58	41.9367	0.02588	0.09162	0.15908	6.37213	0.17057	52.5029	0	0.31833	0	0.0005
31/3.	AL4327-ch5-ol1a	101.38	41.7853	0.00867	0.07308	0.12916	7.11499	0.19565	51.7979	0.02191	0.24546	0	0.0039
31/4.	AL4327-ch5-ol1a	100.89	41.6141	0.01984	0.06438	0.11732	8.43259	0.24106	50.1546	0.0023	0.23167	0.01035	0.0002
31/5.	AL4327-ch5-ol1a	100.93	41.1085	0.02816	0.05236	0.12807	10.8304	0.28414	48.2414	0	0.23631	0.02077	0
	count:	5	5	5	5	5	5	5	5	5	5	5	5
	average:	101.18	41.67	0.02	0.08	0.14	7.72	0.21	51.07	0.01	0.27	0.01	0.00
	stdevp:	0.26	0.30	0.01	0.02	0.02	1.78	0.05	1.66	0.01	0.04	0.01	0.00
32/2.	AL4327-ch5-ol1b	100.83	41.4537	0.03411	0.06963	0.11369	9.53393	0.30733	49.0338	0	0.26122	0.01409	0.005
32/3.	AL4327-ch5-ol1b	100.99	41.453	0.02222	0.05739	0.13645	10.1661	0.37532	48.5545	0	0.22777	0	0
32/4.	AL4327-ch5-ol1b	100.99	41.1776	0.02339	0.04987	0.1275	10.9278	0.39394	48.0345	0.03321	0.21461	0.00233	0.005
	count:	3	3	3	3	3	3	3	3	3	3	3	3
	average:	100.94	41.36	0.03	0.06	0.13	10.21	0.36	48.54	0.01	0.23	0.01	0.00
	stdevp:	0.08	0.13	0.01	0.01	0.01	0.57	0.04	0.41	0.02	0.02	0.01	0.00
	All AL4237-ch2-olivine:												
	count:	8	8	8	8	8	8	8	8	8	8	8	8
	average:	101.09	41.55	0.02	0.07	0.14	8.65	0.26	50.12	0.01	0.26	0.01	0.00
	stdevp:	0.24	0.29	0.01	0.02	0.02	1.89	0.09	1.81	0.01	0.04	0.01	0.00
	Formula:		1.002	0.000	0.002	0.003	0.174	0.005	1.802	0.000	0.007	0.000	0.000
	Mg# = Mg/(Fe+Mn+Mg+Ni+Ca):		**0.91**										
33/2.	AL4327-ch5-opx1a	101.26	58.8776	0.13886	1.01766	1.0251	2.36134	0.22972	37.2535	0	0.35656	0	0
33/3.	AL4327-ch5-opx1a	101.01	58.9181	0.12384	1.00456	1.02993	2.33854	0.22975	36.9907	0	0.36924	0.0039	0.0024
33/4.	AL4327-ch5-opx1a	101.52	59.0852	0.12384	0.95792	1.04056	2.43613	0.24491	37.2412	0.01693	0.37184	0	0
	count:	3	3	3	3	3	3	3	3	3	3	3	3
	average:	101.26	58.96	0.13	0.99	1.03	2.38	0.23	37.16	0.01	0.37	0.00	0.00
	stdevp:	0.21	0.09	0.01	0.03	0.01	0.04	0.01	0.12	0.01	0.01	0.00	0.00
	Formula:		1.975	0.003	0.039	0.027	0.067	0.007	1.856	0.000	0.013	0.000	0.000
	Mg# = Mg/(Fe+Mn+Mg+Ni+Ca):		**0.96**	# = Al/(Si+Ti+Al+Cr):		**0.02**	ง่g# = Mg/(Fe+Mn+Mg+Ni+Ca):			**0.01**			
	All AL4448-ch1-olivine:												
18/1.	AL4448-ch1-ol1a	101.10	40.916	0.06156	0.04582	0.12028	14.3728	0.32408	45.0803	0	0.16372	0.01004	0.0022
18/2.	AL4448-ch1-ol1a	101.39	40.8971	0.05036	0.08094	0.15101	13.3182	0.3309	46.3967	0.02262	0.10241	0.03548	0
18/3.	AL4448-ch1-ol1a	101.37	40.8402	0.01168	0.02359	0.09354	13.4611	0.34423	46.3528	0.03833	0.19186	0.00285	0.0082
18/4.	AL4448-ch1-ol1a	101.36	40.8106	0.04444	0.03379	0.13725	13.4505	0.35361	46.4031	0.01802	0.10112	0.0125	0
18/5.	AL4448-ch1-ol1a	100.86	40.6578	0.02286	0.03363	0.09706	13.5541	0.34664	45.9899	0.01802	0.12083	0.01247	0.0116
	count:	5	5	5	5	5	5	5	5	5	5	5	5
	average:	101.22	40.82	0.04	0.04	0.12	13.63	0.34	46.04	0.02	0.14	0.01	0.00
	stdevp:	0.21	0.09	0.02	0.02	0.02	0.38	0.01	0.51	0.01	0.04	0.01	0.00
	Formula:		1.005	0.001	0.001	0.002	0.281	0.007	1.690	0.000	0.004	0.001	0.000
	Mg# = Mg/(Fe+Mn+Mg+Ni+Ca):		**0.85**										

Table 4: Electron microprobe data, 10 micron beam diameter.

n	Comment	total	SiO2	TiO2	Al2O3	Cr2O3	FeO	MnO	MgO	NiO	CaO	Na2O	**P2O5**
	Ti-, Al-bearing OPX:												
1 / 1 .	AL4327-ch2-x1	101.1948	51.07119	2.34775	12.66136	1.14486	0.48544	0.0826	32.88809	0.03857	0.45504	0.00974	0.01013
3 / 1 .	AL4327-ch2-x3	100.7067	51.2969	2.17893	11.58302	0.96094	0.47783	0.06032	33.47226	0.03284	0.63643	0	0.00723
13 / 1 .	AL4327-ch2-x13	100.724	51.45921	2.37831	11.10862	1.2388	0.50261	0.06014	33.33047	0	0.64145	0.0044	0
17 / 1 .	AL4327-ch2-x17	100.7253	50.40677	1.85906	13.17553	1.2058	0.55058	0.0669	33.00814	0	0.44553	0.00699	0
	count:	4	4	4	4	4	4	4	4	4	4	4	4
	average:	100.84	51.06	2.19	12.13	1.14	**0.50**	0.07	33.17	0.02	0.54	0.01	0.00
	stdevp:	0.21	0.40	0.21	0.82	0.11	**0.03**	0.01	0.24	0.02	0.09	0.00	0.00
	Formula:		1.714	0.055	0.480	0.030	0.014	0.002	1.660	0.000	0.020	0.000	0.000
	Mg# = Mg/(Fe+Mn+Mg+Ni+Ca):		**0.98**	# = Al/(Si+Ti+Al+Cr):		**0.21**	Mg# = Mg/(Fe+Mn+Mg+Ni+Ca):			**0.01**			
	Forsteritic Olivine:												
4 / 1 .	AL4327-ch2-x4	100.7685	42.75229	0.16194	0.076	0.13163	1.26276	0.06157	56.14463	0.00082	0.16682	0.01004	0
5 / 1 .	AL4327-ch2-x5	100.7851	42.90773	0.09332	0.02414	0.05181	1.69412	0.11176	55.70765	0.01508	0.15685	0.00525	0.01735
6 / 1 .	AL4327-ch2-x6	100.9598	42.72294	0.13853	0.07106	0.10604	1.80856	0.11395	55.87315	0	0.1256	0	0
	count:	3	3	3	3	3	3	3	3	3	3	3	3
	average:	100.84	42.79	0.13	0.06	0.10	**1.59**	0.10	55.91	0.01	0.15	0.01	0.01
	stdevp:	0.09	0.08	0.03	0.02	0.03	0.24	0.02	0.18	0.01	0.02	0.00	0.01
	Formula:		1.001	0.002	0.002	0.002	0.031	0.002	1.950	0.000	0.004	0.000	2.995
	Mg# = Mg/(Fe+Mn+Mg+Ni+Ca):		**0.981**										
	Groundmass:												
7 / 1 .	AL4327-ch2-x7	100.312	43.34287	0.00889	36.51746	0.04018	0.1868	0.0127	0.20637	0	19.76925	0.22406	0.00345
8 / 1 .	AL4327-ch2-x8	99.77091	43.80545	0.04284	34.75872	0.01943	**0.56142**	0.01455	**2.04986**	0	18.02198	0.48693	0.00974
9 / 1 .	AL4327-ch2-x9	99.65438	44.54167	0.01412	35.61365	0.03558	0.23978	0	0.23998	0.03517	18.08359	0.85085	0
10 / 1 .	AL4327-ch2-x10	99.80371	44.08977	0.00373	35.80445	0	0.07629	0	0.37567	0.03346	18.8822	0.5304	0.00774
15 / 1 .	AL4327-ch2-x15	100.0894	45.04132	0.03564	34.96253	0.06476	0.18817	0.00213	0.23353	0	18.56998	0.99133	0
	count:	5	5	5	5	5	5	5	5	5	5	5	5
	average:	99.93	44.16	0.02	35.53	0.03	0.25	0.01	0.62	0.01	18.67	0.62	0.004
	stdevp:	0.24	0.59	0.02	0.63	0.02	0.16	0.01	0.72	0.02	0.64	0.27	0.004
	Spinel:												
12 / 1 .	AL4327-ch2-x12	100.4913	0.34092	0.18043	71.44471	0.82109	1.71866	0.02935	25.81581	0	0.13225	0.00806	0
14 / 1 .	AL4327-ch2-x14	101.2953	0.38163	0.44423	69.0229	2.03722	5.08705	0.09567	24.16124	0	0.0529	0.01253	0
16 / 1 .	AL4327-ch2-x16	101.0125	**2.16624**	0.30471	68.88675	1.35846	0.6673	0.05503	27.49011	0	0.05154	0.02454	0.00783
	count:	3	3	3	3	3	3	3	3	3	3	3	3
	average:	100.93	0.96	0.31	69.78	1.41	2.49	0.06	25.82	0.00	0.08	0.02	0.00
	stdevp:	0.33	0.85	0.11	1.18	0.50	1.89	0.03	1.36	0.00	0.04	0.01	0.00
	Formula:		0.023	0.006	1.956	0.026	0.050	0.001	0.916	0.000	0.002	0.001	2.980
	Mg# = Mg/(Fe+Mn+Mg+Ni+Ca):		**0.946**		**Cr and Mn contents highly variable.**								

n	Comment	total	SiO2	TiO2	Al2O3	Cr2O3	FeO	MnO	MgO	NiO	CaO	Na2O	**P2O5**
1 / 1 .	AL4308-chA-x1	101.0177	54.68722	0.54111	22.94938	0.1922	1.68269	0.22397	5.41968	0.03427	11.28261	3.97886	0.02575
4 / 1 .	AL4308-chA-x4	101.0086	54.19345	0.57022	23.2178	0.14467	1.5836	0.21456	5.63296	0.06976	11.39957	3.98196	0
6 / 1 .	AL4308-chA-x6	100.3817	52.64202	0.66795	22.40832	0.24934	2.52991	0.23559	5.86698	0.02357	12.21064	3.5232	0.02415
	count:	3	3	3	3	3	3	3	3	3	3	3	3
	average:	100.80	53.84	0.59	22.86	0.20	1.93	0.22	5.64	0.04	11.63	3.83	0.02
	stdevp:	0.30	0.87	0.05	0.34	0.04	0.42	0.01	0.18	0.02	0.41	0.22	0.01
	Formula:		2.452	0.020	1.227	0.007	**0.074**	0.009	0.383	0.002	0.568	0.338	5.079
		Al - Ca =	**0.659**		Al + Si + Fe =	**3.753**		Ca + Na =	**0.906**				
	Mesostasis:	**This is a glass, viz: High TiO2, MgO; no feldspar or melilite stoichiometry.**											
	Ca-rich pyroxene:												
2 / 1 .	AL4308-chA-x2	100.5345	49.20105	1.03514	9.37089	2.15872	1.72051	0.29483	18.01769	0.00991	18.67449	0.04369	0.00764
3 / 1 .	AL4308-chA-x3	100.3068	49.47741	0.80729	9.4267	2.0847	1.7696	0.3489	18.36382	0	17.95135	0.05217	0.02488
5 / 1 .	AL4308-chA-x5	100.6186	54.19345	1.06658	8.53244	2.25222	1.71594	0.25164	18.51331	0.0403	18.43169	0.04345	0.00834
	count:	3	3	3	3	3	3	3	3	3	3	3	3
	average:	100.49	50.96	0.97	9.11	2.17	1.74	0.30	18.30	0.02	18.35	0.05	0.01
	stdevp:	0.13	2.29	0.12	0.41	0.07	0.02	0.04	0.21	0.02	0.30	0.00	0.01
	Formula:		1.791	0.026	0.377	0.060	0.051	0.009	0.959	0.000	0.691	0.003	3.967
	Mg# = Mg/(Fe+Mn+Mg+Ni+Ca):		**0.561**										
7 / 1 .	AL4308-chA-x7-OL	101.0567	42.54014	0.00679	0	0.08434	5.00279	0.16409	53.05283	0	0.17125	0.01695	0.01749
8 / 1 .	AL4308-chA-x8-OPX	100.9696	58.43897	0.13034	1.51987	0.81582	2.50454	0.13386	36.43613	0.03162	0.91378	0.0447	0

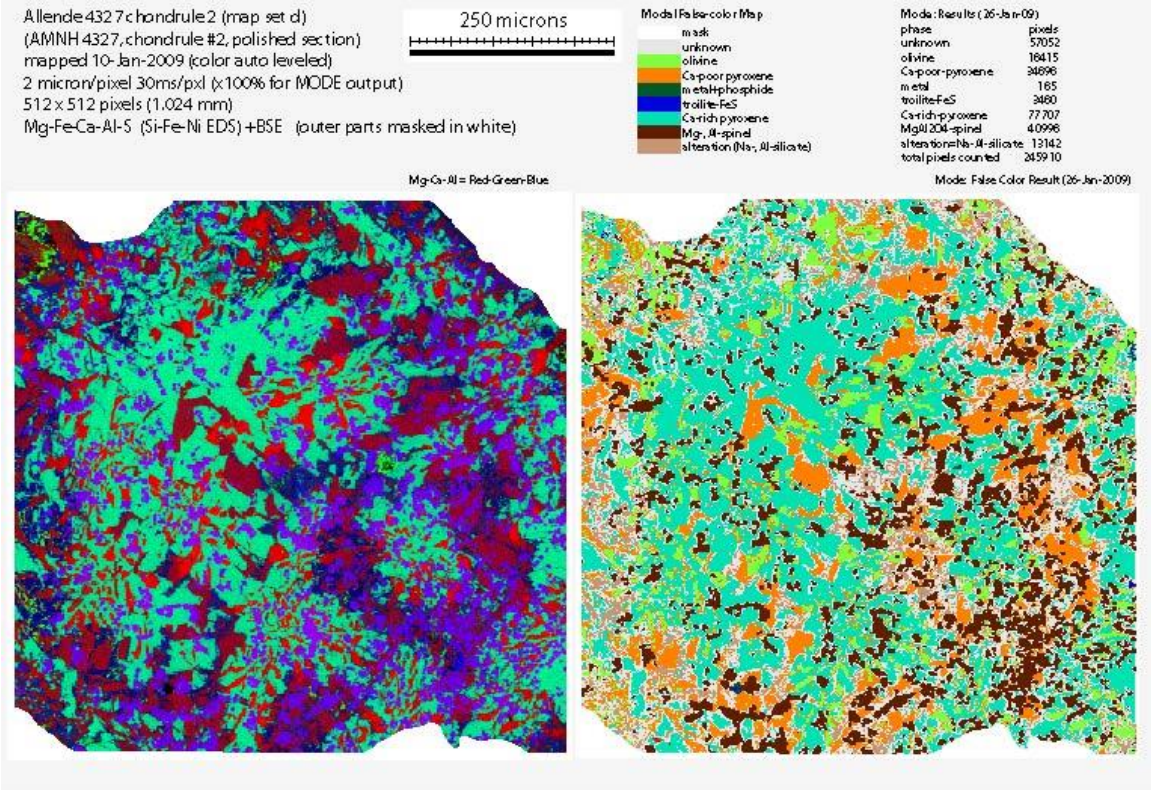

Figure 6: Modal analysis results (right) for 4327-ch2, and Mg-Ca-Al map (left).

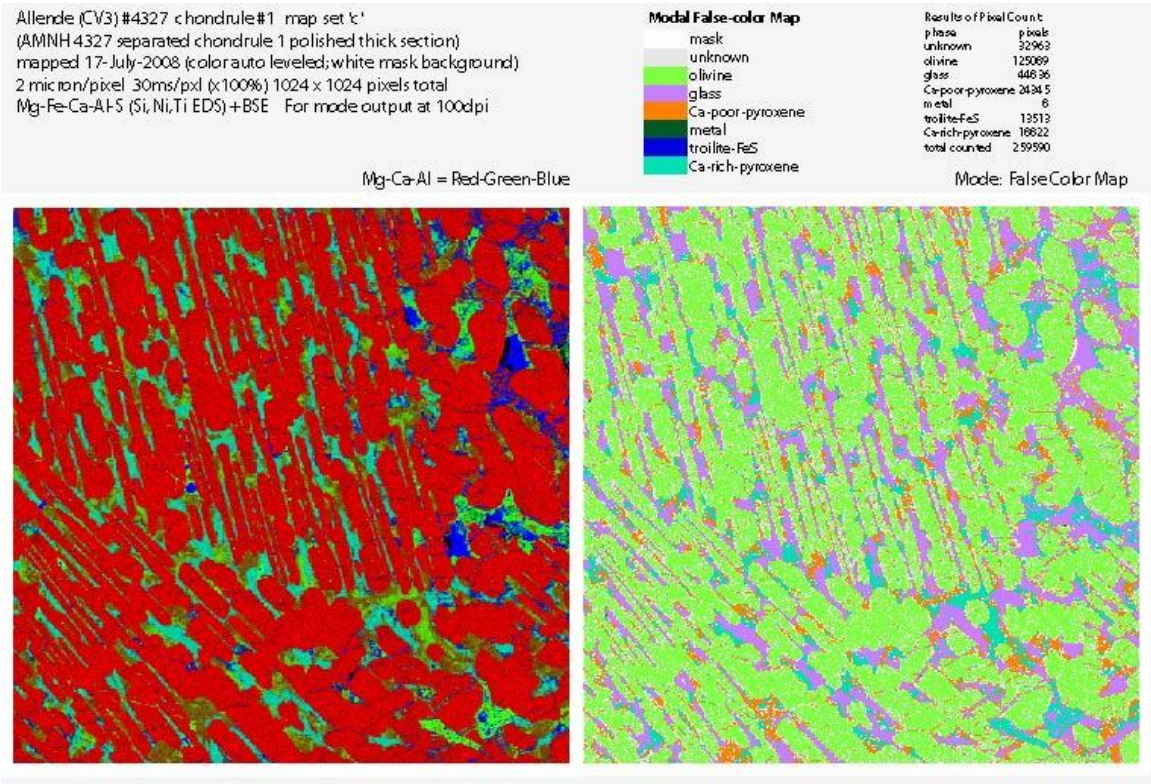

Figure 7: Modal analysis results (right) for 4327-ch1, and Mg-Ca-Al map (left).

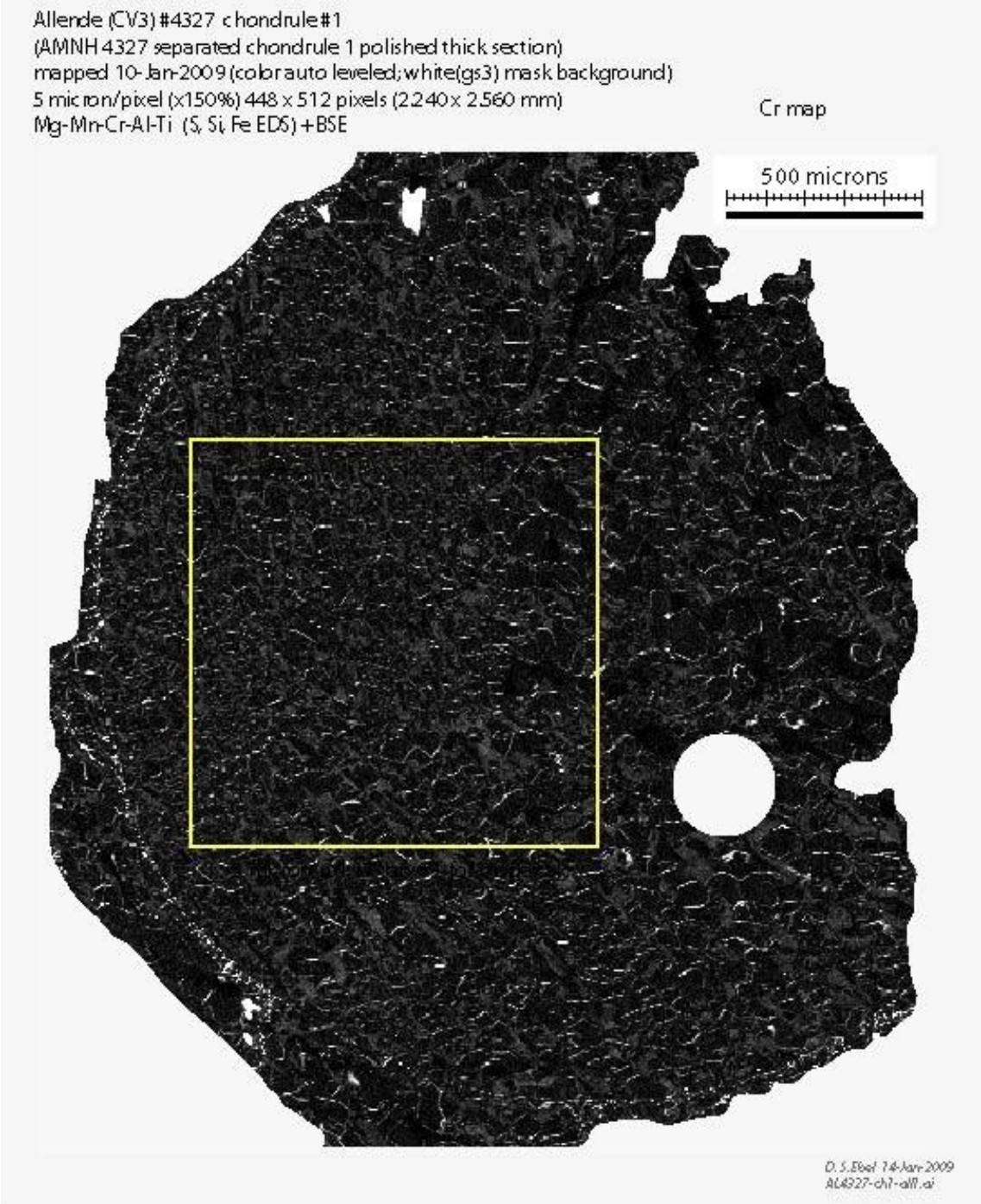

Figure 8: Chromium x-ray map of chondrule 4327-ch1.

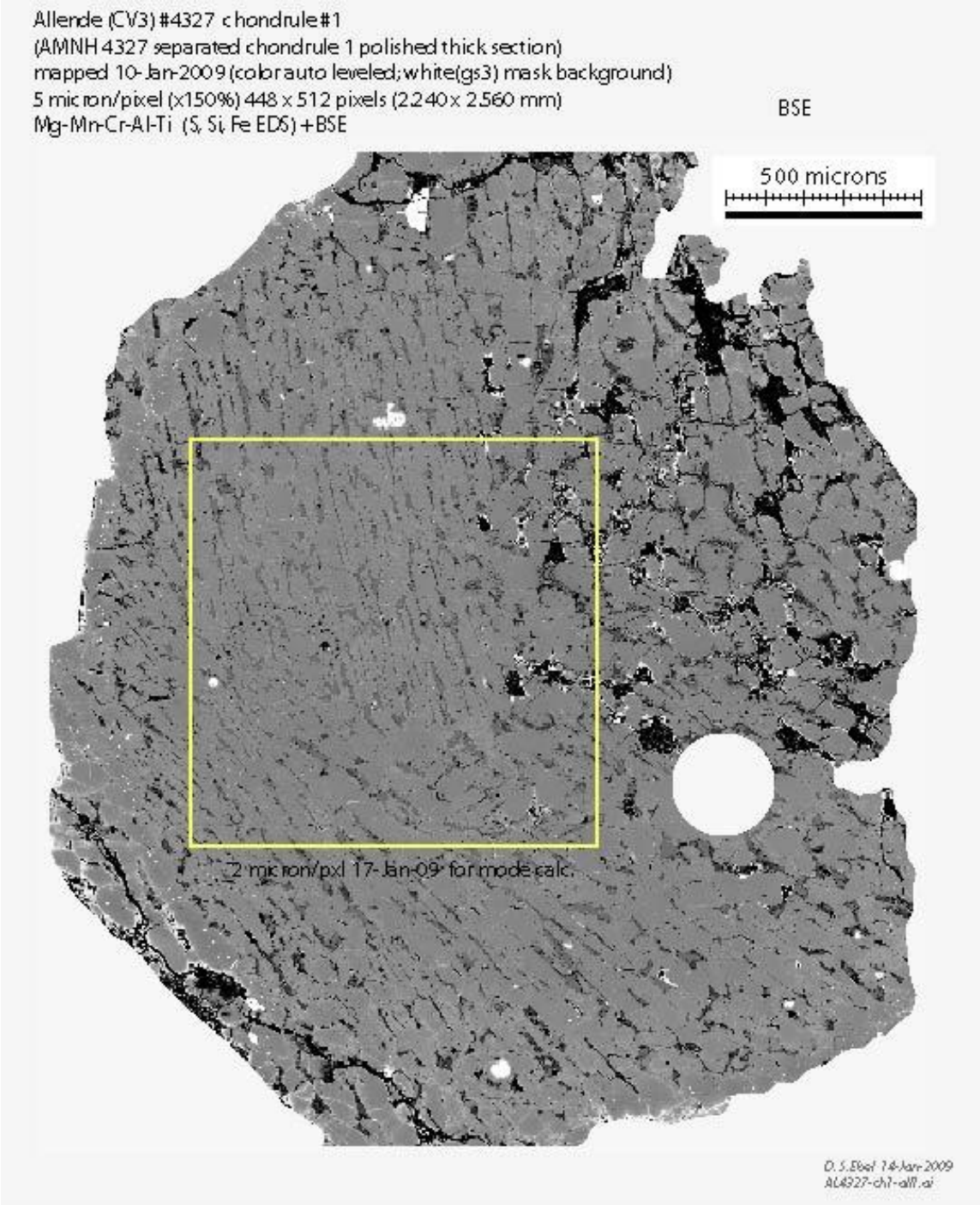

Figure 9: Back-scattered electron (BSE) image of chondrule 4327-ch1.

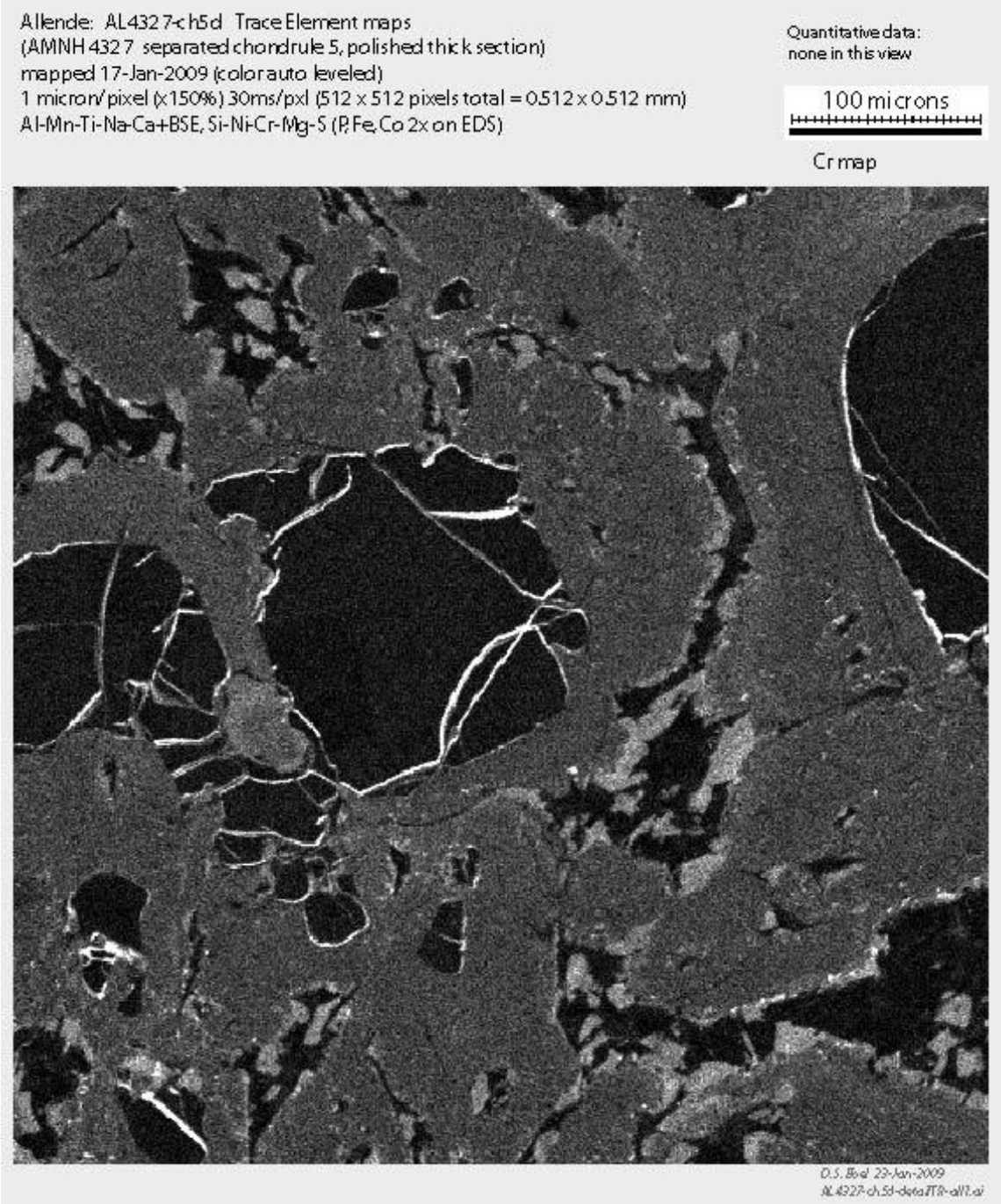

Figure 10: X-ray intensity map of Cr in detail area of chondrule 4327-ch5. Dark phase is olivine.

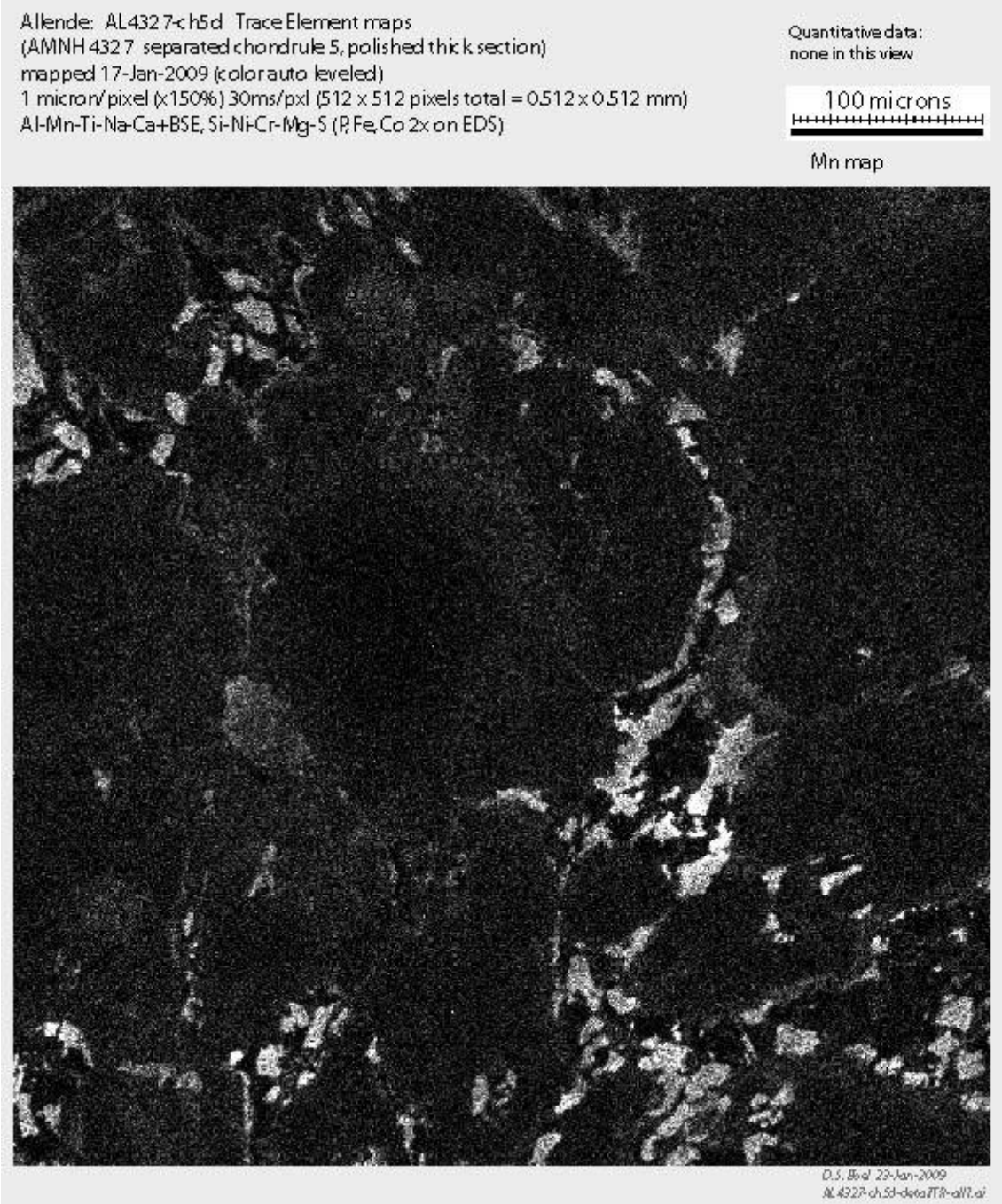

Figure 11: X-ray intensity map of Mn in detail area of chondrule 4327-ch5. Dark phase is olivine.

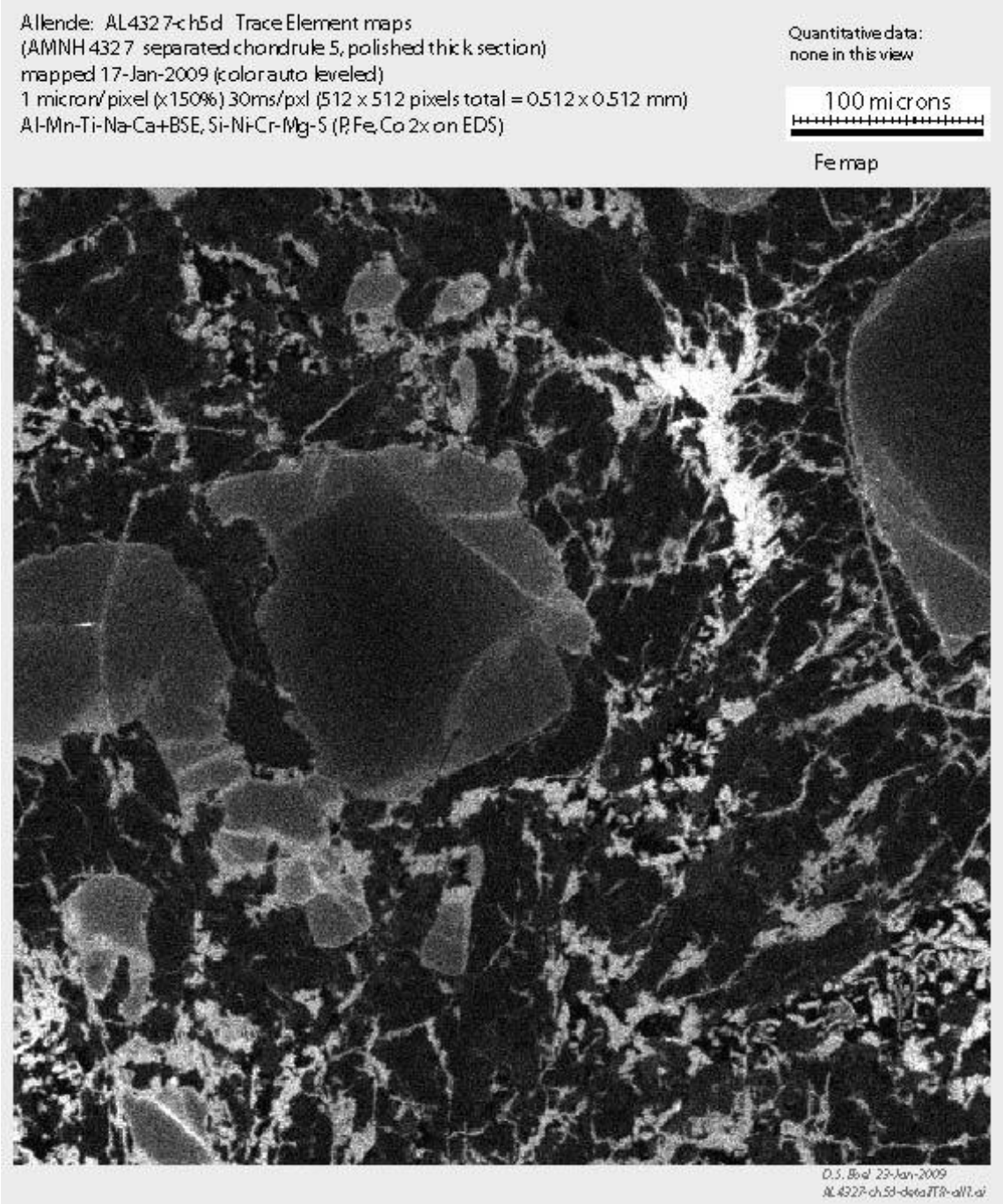

Figure 12: X-ray intensity map of Fe in detail area of chondrule 4327-ch5.

References:

Cameron M. and Papike J.J. (1980) MSA Reviews in Mineralogy Volume 7, *Pyroxenes* (ed. C.T. Prewitt), pp. 5-92;

Ebel D.S., and Rivers M.L. (2007) Meteorite 3-dimensional synchrotron micro-tomography: Methods and applications. *Meteoritics and Planetary Science* **42**: 1627-1646.

Ebel D.S., Weisberg M.K., Hertz J., and Campbell A.J. (2008) Shape, metal abundance, chemistry and origin of chondrules in the Renazzo (CR) chondrite.*Meteoritics and Planetary Science* **43**: 1725-1740.

Ebel D.S., Brunner C., Leftwich K., Erb I., Lu M., Konrad K., Rodriguez H., Friedrich J.M., and Weisberg, M.K. (2016) Abundance, composition and size of inclusions and matrix in CV and CO chondrites. *Geochimica Cosmochimica Acta*, **172**: 322-356. doi: 10.1016/j.gca.2015.10.007 Extended supplement: http://dx.doi.org/10.5531/sd.eps.2

Rivers M.L. (2012) tomoRecon: High-speed tomography reconstruction on workstations using multi-threading. Proccedings of the Society of Photo-Optical Instrumentation Engineers (SPIE) 8506, Developments in X-ray Tomography VIII, 85060U (17 October 2012). https://doi.org/10.1117/12.930022 and https://www.spiedigitallibrary.org/conference-proceedings-of-spie/8506/85060U/tomoRecon--High-speed-tomography-reconstruction-on-workstations-using-multi/10.1117/12.930022.short?SSO=1

Sack R.O. and Ghiorso M.S. (1994) Thermodynamics of multicomponent pyroxenes III: Calibration of $Fe^{2+}(Mg)_{-1}$, $TiAl(MgSi)_{-1}$, $TiFe^{3+}(MgSi)_{-1}$, $AlFe^{3+}(MgSi)_{-1}$, $NaAl(CaMg)_{-1}$, $Al_2(MgSi)_{-1}$ and $Ca(Mg)_{-1}$ exchange reactions between pyroxenes and silicate melts. *Contrib. Mineral. Petrol.* **118**: 271-296.

Sack R.O and Ghiorso M.S. (2017) Ti^{3+}- and Ti^{4+}-rich fassaites at the birth of the solar system: Thermodynamics and applications. *Am. J. Science* **317**: 807-845. DOI 10.2475/07.2017.02

Williams C.D., Sanborn M.E., Defouilloy C., Yin Q-z., Kita N.T., Ebel D.S., Yamakawa A. and Yamashita K. (2020) Chondrules reveal large-scale outward transport of inner Solar System materials in the protoplanetary disk. In press, *Proc. National Academy Sciences*.